JOURNAL OF GEOPHYSICAL RESEARCH, VOL. 115, D02113, doi:10.1029/2009JD012194, 2010

Compatibility between modes of low-frequency variability and circulation types: A case study of the northwest Iberian Peninsula

A. M. Ramos,[1] M. N. Lorenzo,[1] and L. Gimeno[1]

Received 6 April 2009; revised 22 September 2009; accepted 24 September 2009; published 30 January 2010.

[1] Modes of low-frequency variability have a major influence on the variability of the climate system at different temporal and spatial scales. Although the North Atlantic Oscillation explains a substantial portion of the climate variability in Europe, it is also necessary to consider other modes of low-frequency variability, such as the Scandinavian index, the eastern Atlantic or the eastern Atlantic/western Russia indices. Furthermore, the relationship between the modes of low-frequency variability and the climate in Europe cannot be considered to be stable over time. The aim of this paper is to assess the compatibility between the modes of low-frequency variability in Europe (computed using a principal component analysis (PCA)) and local circulation regimes (using an automated version of the Lamb weather-type classification), thus to observe how shifts in the positions of the modes of low-frequency variability in Europe, could affect local circulation. Our study area (NW Iberian Peninsula) was chosen because it is characterized by the passage of cold fronts associated with the storm track in the North Atlantic Ocean and is sensitive to any variability in precipitation and temperature that is linked to the main North Atlantic modes of low-frequency variability. The results show that there is a high degree of correlation between regional modes of low-frequency variability derived from a statistical approach (using PCA) and real physical circulations (as represented by circulation types). Furthermore, changes in the position of modes of low-frequency variability tend to favor some circulation types over others.

Citation: Ramos, A. M., M. N. Lorenzo, and L. Gimeno (2010), Compatibility between modes of low-frequency variability and circulation types: A case study of the northwest Iberian Peninsula, *J. Geophys. Res.*, *115*, D02113, doi:10.1029/2009JD012194.

1. Introduction

[2] Recent observations have highlighted the fact that significant climate trends are evident at different time scales over the North Atlantic–European (NAE) sector [*Intergovernmental Panel on Climate Change*, 2007; *Trigo et al.*, 2008]. The variability in atmospheric circulation is the most important issue in terms of the changes in the spatial distribution, not only of temperature or precipitation, but also of other climatological variables.

[3] A distinctive characteristic of the interannual variability of large-scale circulation patterns is the degree to which they are organized spatially, as represented by their modes of low-frequency variability. These patterns, which are considered by many authors to be the preferred modes of low-frequency variability of atmospheric circulation, consist of in-phase or out-of-phase variations of geopotential or sea level pressure in areas normally termed "centers of action." Modes of low-frequency variability are concepts for understanding the complex relationship between planetary-scale circulation and regional climate, including the occurrence of extreme events.

[1]EPHYSLAB, Faculty of Sciences, University of Vigo, Ourense, Spain.

0148-0227/10/2009JD012194$09.00

[4] The first major studies to refer to modes of low-frequency variability were those of *Wallace and Gutzler* [1981] for the winter period and *Barnston and Livezey* [1987] for all seasons. For the NAE sector, the most prominent patterns according to *Barnston and Livezey* [1987] are the North Atlantic Oscillation (NAO), east Atlantic pattern (EA), Eurasian pattern 1 (also referred as east Atlantic/western Russia pattern (EA/WR)) and Eurasian pattern 2 (also referred as the Scandinavian pattern (SCA)). Over the last two decades, several studies have assessed the impact of these modes on the European climate (in particular on temperature and precipitation). The NAO is the main modes of low-frequency variability in the NAE sector and is correlated with the surface climate in most of the European region [*Hurrell and van Loon*, 1997; *Lu and Greatbatch*, 2002; *Trigo et al.*, 2002; *Jones et al.*, 2003; *Bojariu and Gimeno*, 2003]. For example, positive NAO index during winters are associated with a northward shift in the Atlantic storm activity, with enhanced activity from southern Greenland across Iceland into northern Europe and a modest decrease in activity to the south, which cause drier conditions to southern Europe [*Hurrell et al.*, 2003].

[5] However, this relationship between the NAO and the climate in Europe cannot be considered to be fully stable. *Chen and Hellström* [1999] pioneered the study of the nonstationarity of circulation-to-weather links in Europe. A number of other studies also note the nonstationary nature

of this relationship, in terms of not only surface temperature [*Slonosky et al.*, 2001; *Gimeno et al.*, 2003,] or sea surface temperature [*Walter and Graf*, 2002], but also precipitation [*Zveryaev*, 2006; *Beranová and Huth*, 2007]. *Jung et al.* [2003] were the first to suggest that the reason for the nonstationarity of the relationship between the variability modes and surface weather was in the changing positions of the action centers of the NAO. In a recent study, *Vicente-Serrano and López-Moreno* [2008] emphasized that the nonstationary relationship between the NAO and precipitation is linked to interdecadal variability in the position of the NAO pressure centers. Moreover, the spatial configuration of the NAO changes substantially prior to the occurrence of clear shifts in the magnitude and spatial distribution of its influence on precipitation patterns in Europe.

[6] Although the NAO is known to be the main modes of low-frequency variability of the Northern Hemisphere that influences the European climate, some studies have also focused on the influence of other modes of low-frequency variability on the NAE sector. The reports include those on precipitation [e.g., *Rodríguez-Puebla et al.*, 1998; *Wibig*, 1999; *Blackburn and Hoskins*, 2001], on the impact on river flow [*Lorenzo and Taboada*, 2005] and on the upwelling intensity [*deCastro et al.*, 2008]. Relationships between other modes of low-frequency variability over the NAE and temperature may also be found in the work of *Sáenz et al.* [2001] and *Beranová and Huth* [2008].

[7] Studies of the temporal variability of the effects of other modes of low-frequency variability also conclude that the relationship between these other modes of low-frequency variability (apart from the NAO) and temperature and precipitation also varies in time and space [*Krichak and Alpert*, 2005; *Beranová and Huth*, 2008].

[8] At the same time, their significance also varies seasonally, tending to be stronger during some seasons than others. For example, the NAO is more pronounced during winter and less clear during the summer months [*Corte-Real et al.*, 1995; *Trigo and Palutikof*, 2001]. In general, the impact of the major modes of low-frequency variability (especially those with zonal dipoles) on precipitation in Europe is higher and more pronounced during the winter months [*Glowienka-Henze*, 1990; *Dunkeloh and Jacobeit*, 2003], when the baroclinity is higher in the extratropical latitudes than it is during the summer. In this paper, we therefore present results only for the winter months, despite having performed analyses for other seasons as well.

[9] One further method used for studying the effects of changes in circulation patterns on regional climate is the estimation of changes in these patterns. Circulation patterns are specific to a given region and result from the examination of synoptic weather data, usually on a regular grid, obtained using a wide variety of methodologies [*Huth et al.*, 2008]. Circulation types are usually defined for each day and tend to reflect the local circulation that actually occurs in a simple way. In contrast, the modes of variability are estimated at a larger temporal and spatial scale than the circulation types and are characterized by a recurring and persistent, large-scale pattern of pressure that covers vast geographical areas. Modes of low-frequency variability reflect large-scale changes in the atmospheric wave and jet stream patterns and they are generally defined by means of principal component analysis. Therefore the circulation field at each time can be approximated by a linear combination of several modes of low-frequency variability. In this way, there is no reason to suppose that the modes of low-frequency variability resemble individual circulation patterns.

[10] In the study reported herein, we used an automated version of synoptic circulation types that was initially developed for the British Isles [*Jones et al.*, 1993] and that describes the local circulation in terms of the circulation parameters, in this case, the mean flow and shear vorticity. Nowadays, the classification of synoptic weather situations gains added importance within the context of the European Cooperation in Scientific and Technical Research (COST) Action (COST 733 – http://www.cost733.org), the main objective of which is to devise a general numerical method for assessing, comparing, and classifying weather situations in Europe that can then be applied to any European (sub)region.

[11] The main aims of this paper are to assess the compatibility between the modes of low-frequency variability and regional circulation patterns and to determine to what extent changes in intensity or shifts in position of the modes of low-frequency variability also influence changes in local circulation.

[12] The region selected for this study is Galicia, in the northwest Iberian Peninsula. It is characterized by the passage of cold fronts associated with the storm track in the North Atlantic Ocean [*Trigo*, 2005]. There are three main reasons for selecting this region. First, previous studies have shown that the precipitation and temperature variability is linked to the main North Atlantic modes of low-frequency variability, i.e., not only the NAO, but also the SCA and EA/WR [*Lorenzo and Taboada*, 2005; *deCastro et al.*, 2006]. Second, this region has suffered from a significant decrease in precipitation over the last 40 years, especially during the winter [e.g., *Paredes et al.*, 2006; *Trigo et al.*, 2008]. Third, the circulation type methodology used here has been applied successfully to the Iberian Peninsula in several other studies, especially those relating to precipitation, e.g., those of *Trigo and DaCamara* [2000] and *Lorenzo et al.* [2008].

[13] The remainder of the paper is organized as follows. In section 2, we describe the different data sets and the methodologies used in their analysis. In section 3, we describe the synoptic circulation types briefly. In section 4, we introduce the concept of modes of low-frequency variability, computed using principal component analysis (PCA) for sea level pressure and 500 hPa geopotential height fields, and their relationship to circulation type. In section 5, the nonstationary nature of the modes of low-frequency variability and its influence on the frequency of each circulation type are discussed. Section 6 concludes.

2. Data Sets and Methodology

[14] The main database that we used consists of daily sea level pressure (SLP) retrieved from NCEP/NCAR reanalysis data [*Kalnay et al.*, 1996]. We used daily winter (January, February and March, hereafter JFM) SLP fields from 1948 to 2005 with a grid size of 2.5°. The spatial window covers the area 30°N–76°N and 37°W–56°E, this being the largest of the regions in the COST 733 initiative.

[15] In this study, we used four different sets of data, in which three corresponding to different methods of quantifying atmospheric circulation variability (sections 2.1–2.3) and

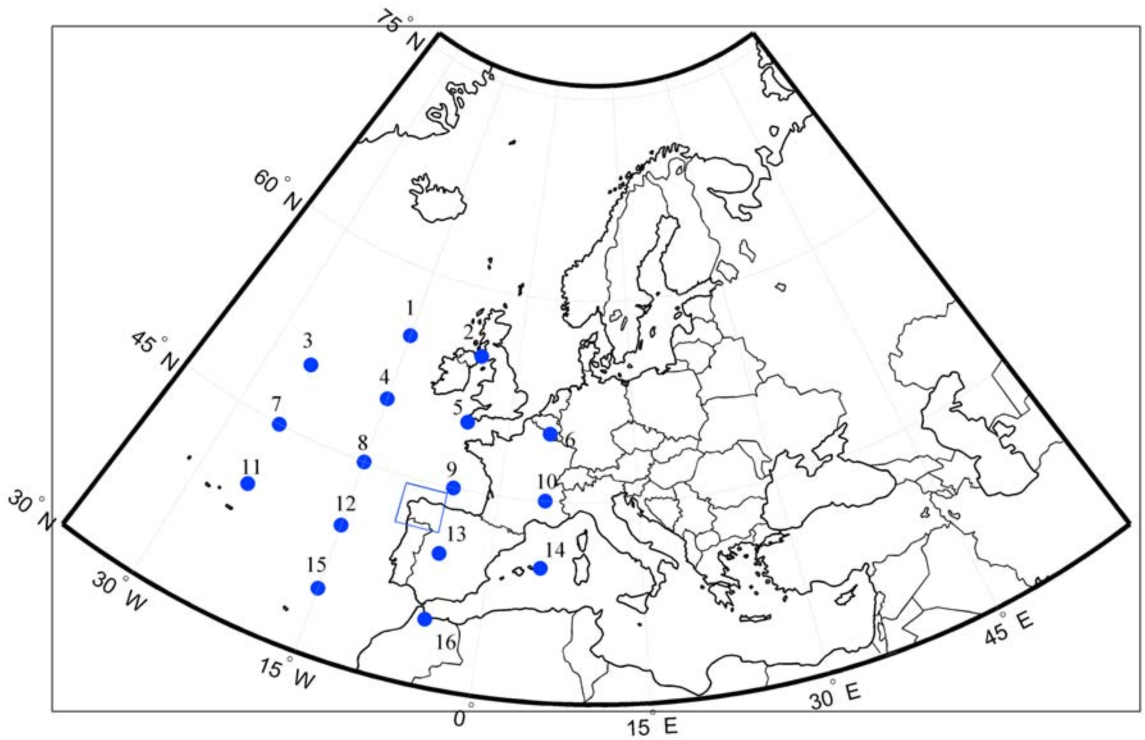

Figure 1. North Atlantic–European domain with the location of the target area (indicated by the square).

one corresponding to the identification of the nonstationary modes of low-frequency variability in the NAE sector (section 2.4).

2.1. Daily Circulation Type Classification

[16] The classification used herein is an automated version of the Lamb weather type procedure [*Jones et al.*, 1993]. In recent years, this method has successfully been applied to other European regions [*Goodess and Palutikof*, 1998; *Trigo and DaCamara*, 2000]. A comprehensive study linking these circulation types to northern hemisphere modes of low-frequency variability and their influence on precipitation in Galicia was carried out by *Lorenzo et al.* [2008].

[17] We used the daily circulation types database that was computed for Galicia by *Lorenzo et al.* [2008]. These circulation types were computed on the basis of the daily SLP retrieved from the NCEP/NCAR reanalysis data [*Kalnay et al.*, 1996]. The circulation conditions were determined using physical or geometrical parameters, such as the direction and strength of airflow, and degree of cyclonicity based on 16 grid points (Figure 1). We only used 10 circulation types, eight driven by the direction of the flow (NE, E, SE, S, SW, W, NW, and N) and two by the shear vorticity (cyclonic or anticyclonic). A comprehensive description of this methodology may be found in Appendix A. Data were obtained only for the winter season (JFM) for the years from 1948 to 2005.

2.2. Hemispheric Modes of Low-Frequency Variability

[18] The standard NAO, EA, EA/WR, and SCA modes of low-frequency variability indices were obtained from the Climate Prediction Center (CPC) of the National Oceanic and Atmospheric Administration (NOAA) for the years 1950–2005 (http://www.cpc.noaa.gov/data/teledoc/telecontents.shtml). These modes of low-frequency variability indices were computed from the 500 hPa geopotential height field for the entire Northern Hemisphere (20°N–90°N), using rotated PCA [*Barnston and Livezey*, 1987]. It is important to note that hereafter the hemispheric modes of low-frequency variability ((NAO, EA, EA/WR, and SCA) are referred as hemispheric modes.

2.3. Stationary Modes of Low-Frequency Variability in the NAE Sector

[19] The PCA technique is one of the most commonly applied to the detection of modes of low-frequency variability and has been used in a variety of climatological studies [e.g., *Jolliffe*, 1990; *Corte-Real et al.*, 1999; *Wibig*, 1999; *Huth*, 2006; *Zveryaev*, 2006]. In order to identify the modes of low-frequency variability in the NAE sector, a PCA technique was carried out. Here we use the same methodology as *Barnston and Livezey* [1987] but with two differences: (1) we use daily fields and (2) we only take into account the NAE sector (30°N–76°N and 37°W–56°E). A comprehensive description of this methodology may be found in Appendix A. The PCA technique was applied to the daily winter (JFM) SLP field and to the daily 500 hPa geopotential height field (H500), for the whole period of analysis (1948–2005). Hereafter, the modes of low-frequency variability will be named "modes," differing only in the height level at which the PCA was computed (SLP modes or H500 modes).

2.4. Identification of the Nonstationary Modes of Low-Frequency Variability in the NAE Sector

[20] In order to identify changes in the modes over time for the winter months (JFM) in the NAE sector, we computed a moving window PCA (with a 30 year period) for JFM, which allowed us to study not only the changes in the spatial

patterns over time but also the changes in position and intensity of the modes. The methodology and spatial domain used to compute the 30 year period PCA was the same as the one described in section 2.3). The first period used in the PCA was 1948–1977 (using 1962 as the central year), the next period was 1949–1978, and so on until the final period 1976–2005 (using 1990 as the central year).

[21] In sections 4 and 5, several correlation analyses are made. In order to so, we create new time series. This time series are seasonal (DJF) and they are averages from daily time series (in the case of the modes and frequency of the circulation types) and from monthly time series (in the case of the hemispheric modes).

3. Synoptic Circulation Types for Galicia

[22] In order to better understand the nature of each circulation type in the study area, we computed composite maps for each one for the period 1950–2005 (Figure 2). In this study, our aim was not to describe each type exhaustively; readers who require further information on this technique are referred to Appendix A.

[23] In Figure 3, we show the frequency of the circulation types observed during the winter months. The most obvious result is that on winter days, the circulation type that has the greatest frequency of occurrence is anticyclonic circulation, which occurs on about one third of the days analyzed. The circulation types driven by airflow from a westerly direction (i.e., NW, W and SW) have higher frequency (6.2%, 17.2%, and 13.6%, respectively) than the eastern circulation types (less than 5% each). Cyclonic circulation types occur on about 10% of the winter days that were analyzed.

4. Compatibility Between Local Circulation Type Classification and Modes of Low-Frequency Variability in the NAE Sector

[24] The Lamb classification of weather types is an important tool used for the study of the daily synoptic variability of a given region. However, in most cases, these daily local circulations are related to the modes. In order to investigate this influence, we computed the PCA, not only for the winter (JFM) SLP field in the NAE sector, but also for the 500 hPa geopotential height field in our area of study (30°N–76°N and 37°W–56°E).

[25] For both the SLP and H500 fields, the four main empirical orthogonal function (EOF) patterns and the respective variance explained by each, in winter, are shown in Figure 4 and Figure 5, respectively. At first glance and on the basis of mere visual comparison, the results for both fields seem very similar. For the first two EOFs the same pattern appears for both fields, while those of EOF 3 and EOF4 are switched between them, i.e., the pattern of EOF3 in the SLP field corresponds to that of EOF4 in the H500 field and that of EOF4 in the SLP corresponds to that of EOF3 in the H500 field. Despite the strong resemblances in the two fields, correlations between the time series of the SLP and H500 modes were computed to provide a more thorough comparison (Table 1a). The results support the visual resemblances with high correlations (significant at a 1% level) between the first two correspondent modes (SLP and H500). Regardless of the change in the positions of the patterns of EOF3 and EOF4 with respect to explained variance in the SLP and H500, when analyzing the cross correlation between them, there were high correlations in both cases, more than 0.92 (significant at 1% level).

[26] In order to put these modes into context, we also computed the correlations between the time series of the modes and the hemispheric modes (NAO, EA, EA/WR and SCA – section 2.2). The results are presented in Tables 1b and 1c. For both climate modes (SLP and H500 field), the first principal component (PC) has the highest correlation (0.77 and 0.75) with the NAO. For the second PC, the highest correlations are with SCA for both fields. In the case of the third PC, for the SLP field it has the highest correlation with the NAO pattern and for the H500 field it has the highest correlation with EA/WR. In contrast, for the fourth PC, the SLP-PC is highly correlated with EA/WR and for the H500 field it has the highest correlation with the NAO. For the third and fourth PCs, this correlation structure was as expected, because of the change in the position of EOF3 and EOF4 with respect to the explained variance in the SLP and H500 fields. These results show that, in general, for our spatial window, there is a one-to-one correspondence between the modes at SLP and H500. Given that the types of circulation that we consider in this work are based on the surface fields, from now on, we will only focus on the SLP field modes. We now describe briefly the four leading modes in the NAE sector for the SLP field (Figure 4) and provide our own nomenclature for naming the modes.

[27] The first EOF (EOF 1), a continental zonal dipole (CZD), explains about 30% of the total variance and is characterized by the presence of strong centers in Scandinavia (negative) and in the Iberian Peninsula (positive), these being separated by a strong north-south gradient. This mode is similar in structure to the NAO pattern (it has a 0.77 correlation with it) but with some influence of the SCA pattern since the correlation between the PC-CZD and SCA are also important (−0.69).

[28] EOF 2 is a continental meridional dipole (CMD), which is characterized by two large-scale structures, with their main centers of action over the Atlantic region and over western Europe. It accounts for 22% of the explained variance. This mode may be associated with the type 1 Eurasian pattern (EU1) described by *Barnston and Livezey* [1987], also known as the Scandinavian pattern (SCA). From Table 1b we can see that it presents higher correlation with the SCA (−0.54 and significant at a 5% level).

[29] EOF 3 is an ocean zonal dipole (OZD), which resembles the NAO pattern. The most important difference is that the OZD is northward shifted when comparing with the NAO. Besides that, it also extends more over western Europe and therefore has a larger horizontal scale. It accounts for 21% of the total variance. This mode has the maximum and minimum values of the centers of action located over Greenland and the Azores region, respectively, favoring a high correlation value with the NAO (−0.83).

[30] EOF 4 is an ocean meridional dipole (OMD) and accounts for 12% of the total variance. This pattern has a main (positive) center located between the British Isles and Denmark. It has two other centers, which are located to the northwest of the Azores Islands and over northern Russia. This pattern bears some resemblance to the type 2 Eurasian pattern (EU2) described by *Barnston and Livezey* [1987],

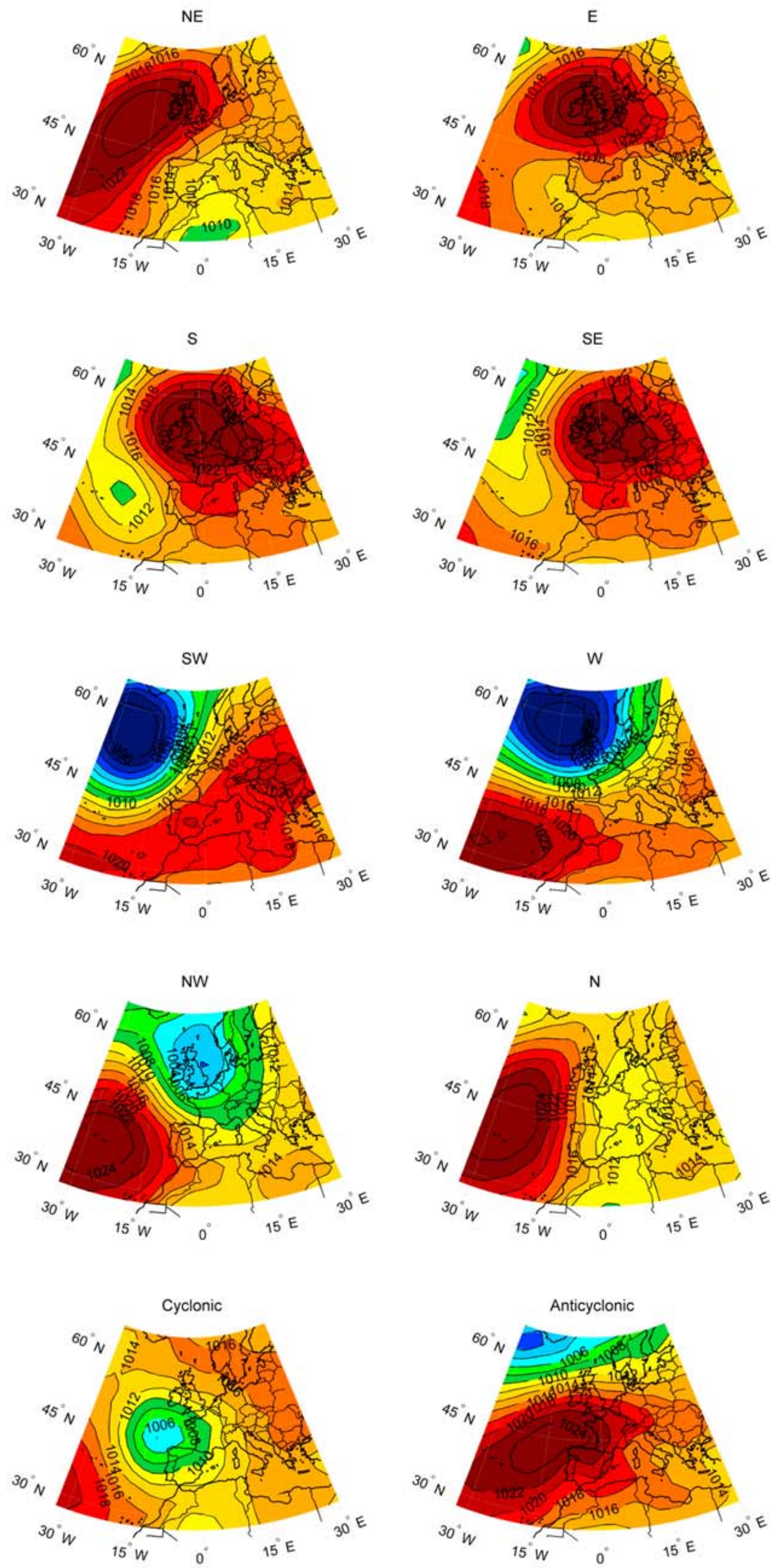

Figure 2. The average of January–February–March (JFM) sea level pressure (SLP) (hPa) field that characterizes the 10 weather types used in this work.

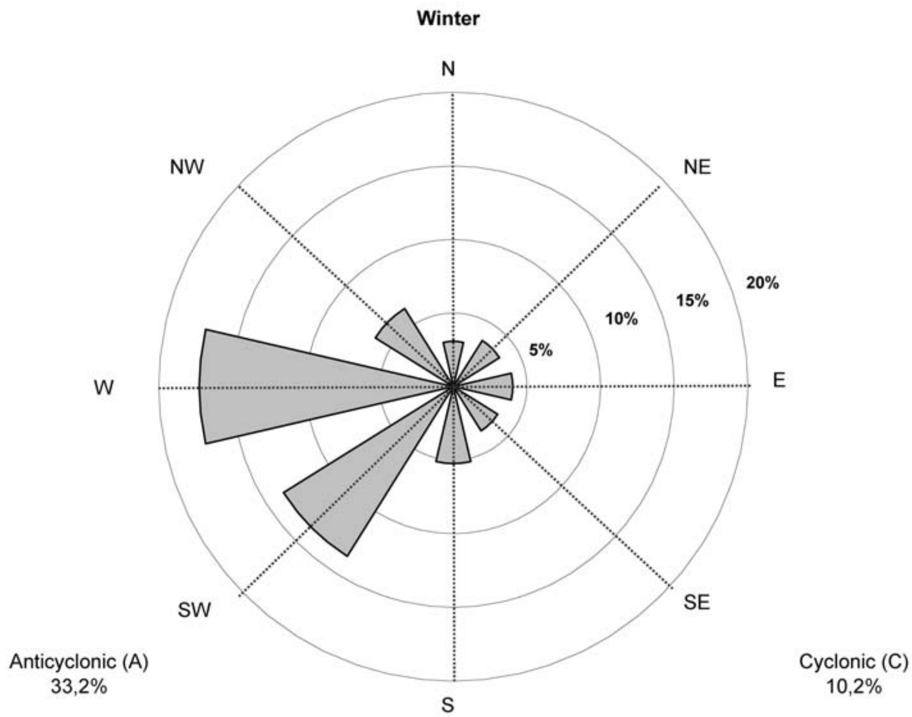

Figure 3. Frequency (%) of circulation types in winter months (JFM).

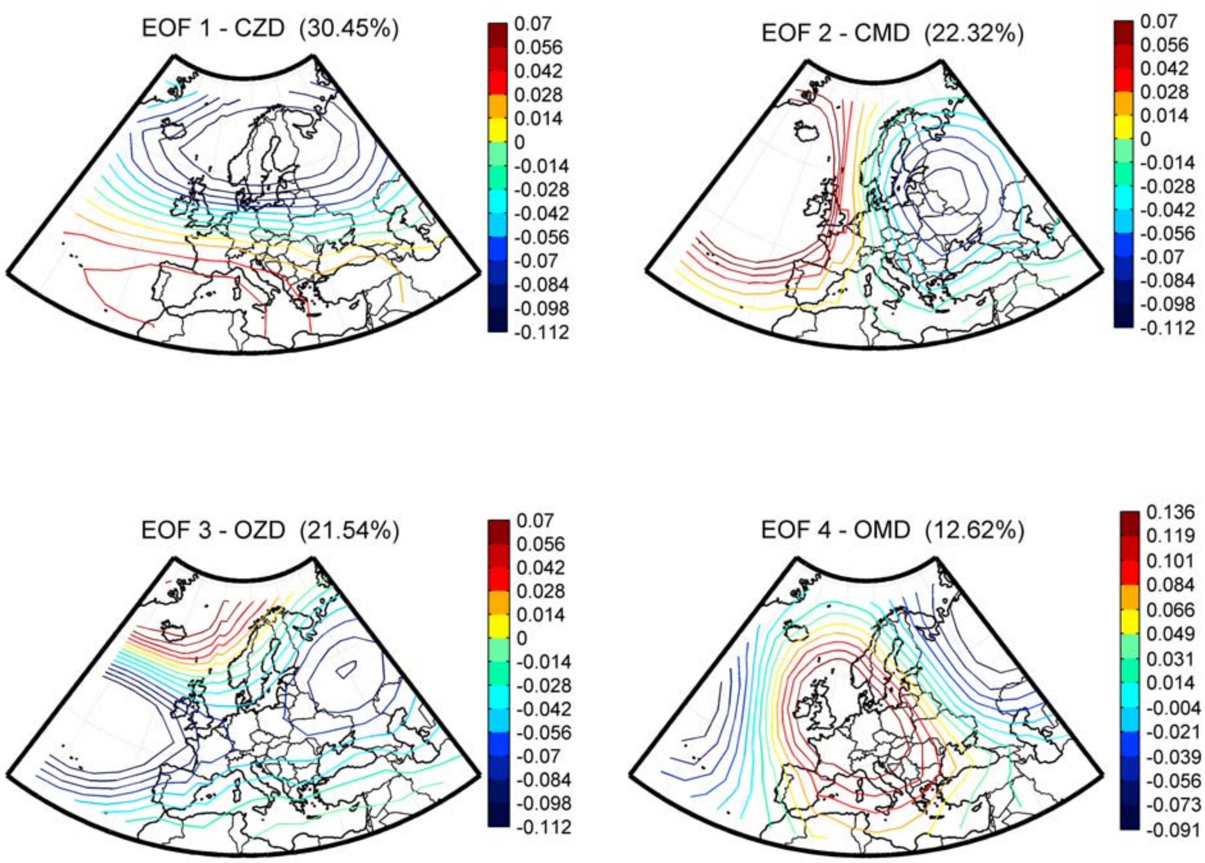

Figure 4. The first four leading empirical orthogonal function (EOF) patterns for the winter months (JFM) for the SLP field together with the respective variance (%) explained by each.

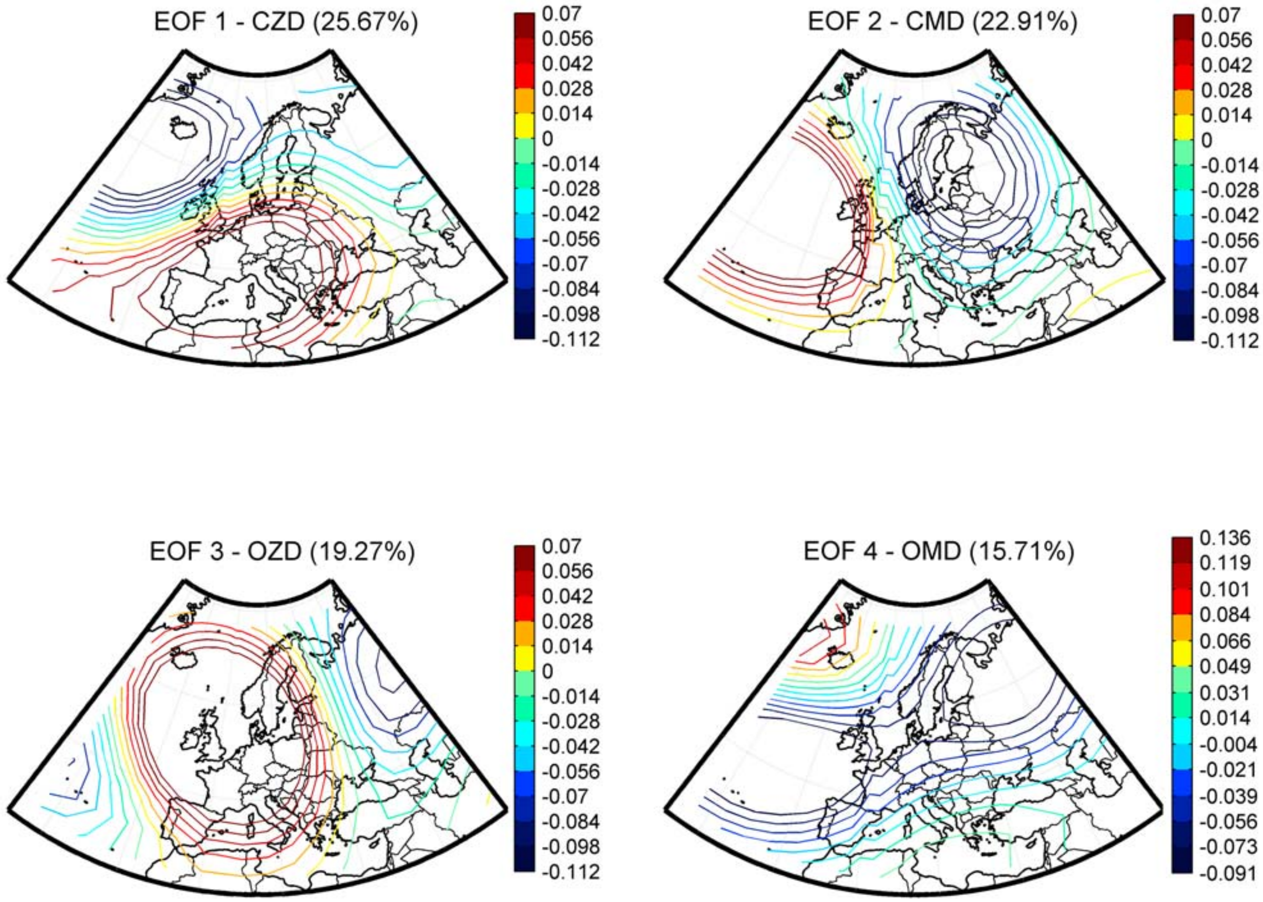

Figure 5. The first four leading EOF patterns for the winter months (JFM) for the H500 field together with the respective variance (%) explained by each.

which is also referred to as the east Atlantic/west Russia (EA/WR) pattern using the terminology of the Climate Prediction Centre of the NOAA. In fact, this mode presents the highest correlations with the EA/WR (0.72).

[31] We provide strong evidence that the modes computed from the SLP field or the H500 field are very alike in this spatial window. Despite this, there is not an obvious one-to-one correspondence between the SLP/H500 modes and the hemispheric modes. This lack of correspondence can be explained by the different methodologies (atmospheric levels, domain, time period, rotation) used when computing the PCA and was also discussed in others studies [e.g., *Beranová and Huth*, 2008; *Jolliffe*, 2002]. In our particular case, the most obvious result is that, EA is missing in the modes computed for this spatial window. The most probable explanation for this is the selection of the domain. EA is described by *Barnston and Livezey* [1987] as a center near 55°N, 20°W–30°W with a strong northwest-southeast gradient over western Europe and an oppositely signed anomaly band over 25°N–35°N, 0W°–10°W. Since our domain is limited to 30°N–76°N we believe that is why this mode is missing in our analysis. It is also interesting to note that the absence of EA pattern is compensated by another NAO like pattern (OZD) maybe in part because of the EA pattern is also structurally similar to the NAO pattern but with the anomaly centers displaced southeastward.

[32] Now that we have characterized the modes in our domain, it is our intention to evaluate the links between the Galician circulation types and the modes. First, we will focus on the major hemispheric modes (section 2.2) that affect the

Table 1a. Correlation Between the Hemispheric Modes Time Series and the Time Series of the Empirical Orthogonal Function Computed for the Sea Level Pressure Field[a]

SLP	NAO	EA	EA/WR	SCA
PC1	**0.7704**	**0.2853**	0.2017	**−0.6919**
PC2	−0.1466	**−0.4079**	0.0803	**−0.5374**
PC3	**−0.8291**	0.0756	−0.0849	0.0377
PC4	**0.2979**	**0.2763**	**0.7238**	**−0.4019**

[a]PC, principal component; SLP, sea level pressure; NAO, North Atlantic Oscillation; EA, east Atlantic pattern; EA/WR, east Atlantic/western Russia pattern; SCA, Scandinavian pattern. Values in bold represent correlations that are statistically significant at the 99% level.

Table 1b. Correlation Between the Hemispheric Modes Time Series and the Time Series of the Empirical Orthogonal Function Computed for the H500 Field[a]

H500	NAO	EA	EA/WR	SCA
PC1	**0.7536**	**0.4744**	0.2176	**−0.5461**
PC2	0.2278	**−0.3391**	0.1623	**−0.7206**
PC3	0.0581	0.1503	**0.7622**	−0.2149
PC4	**−0.7884**	0.0424	0.0143	−0.0556

[a]Values in bold represent correlations that are statistically significant at the 99% level. H500 refers to 500 hPa geopotential height.

Table 1c. Correlation Between the Times Series of Both Empirical Orthogonal Function Fields Computed for Our Region of Study[a]

	H500			
SLP	PC1	PC2	PC3	PC4
PC1	**0.9103**	**0.4982**	0.1439	**−0.4666**
PC2	−0.1847	**0.8663**	0.1633	0.0327
PC3	**−0.4130**	**−0.3106**	−0.2054	**0.9264**
PC4	**0.4017**	**0.2899**	**0.9209**	−0.2359

[a]Values in bold represent correlations that are statistically significant at the 99% level.

dominant patterns of variability of atmospheric circulation in Galicia (Table 2). Second, we will reduce the spatial domain and focus on the modes in the NAE sector (Figure 4 and Figure 5). Given that we have already demonstrated the relationship between hemispheric modes and the modes in the NAE sector, the first issue will be considered only briefly.

[33] Table 2 shows the coefficients obtained from the correlation between the four large-scale hemispheric modes and the frequency of the 10 circulation types during the winter months (JFM). As expected, the most significant correlations are those obtained between the NAO and the frequency of cyclonic and anticyclonic circulation types. This inverse correlation with the frequency of cyclonic type is in line with the decrease in the occurrence of storm tracks in the region when the NAO is in its positive phase [*Trigo*, 2005]. The EA index also shows high correlations with the frequency of SW circulation type, which is the third most frequent type occurring in winter. The EA/WR index shows a fairly high correlation with the frequency of W, NW, and SE circulation types. In addition, the SCA index exhibits a pattern of behavior that is the opposite of the NAO, showing a high negative correlation with the frequency of anticyclonic type and a high positive correlation with the frequency of cyclonic circulation type.

[34] Finally, we discuss the relationship between the circulation type and the modes in the NAE sector, using the SLP four leading PC loading factors. For each day, we carried out an objective comparison between the four leading PC loading factors and the daily local circulation type in the study area. By combining the corresponding daily circulation type with the four PCs we were able to compute, for each circulation type, the statistical distribution of the PCs. The results are summarized in Figure 6. Here, we call the four leading PC loading factors PC-CZD, PC-CMD, PC-OZD, and PC-OMD, respectively. The boxes in Figure 6 show the lower, median, and upper quartile values, respectively. The whisker lines are also shown and are drawn to 1.5 times of the interquartile range. For the first PC (PC-CZD), the most striking result is the difference between the cyclonic (negative index for PC-CZD) and anticyclonic circulation type (positive index for PC-CMD), which are in line with the results for the storm track in Iberia [*Trigo*, 2005; *Garcia-Herrera et al.*, 2007] and the ones presented in Table 2. It is interesting to note that the circulation types that are driven by the direction of flow (see section 2.1) tend to occur with a negative PC-CZD index. Because of the nature of the strong north-south gradient of the CZD pattern, the indices of the W and E types are opposite in sign.

[35] The strong west-east gradient in the CMD pattern in the Iberian Peninsula influences some of the directional circulation types, especially those from NE, E, SW and W, where an opposite distribution may clearly be seen (compare NE and E versus SW and W). There is no apparent difference between the cyclonic and anticyclonic types in the CMD pattern.

[36] For PC-OZD, the only very clear point to note is, once again, the difference in sign between the cyclonic (positive index for PC-CZD) and anticyclonic circulation type (negative index for PC-OZD). Given that the CZD and OZD share some common characteristics but are opposite in sign (see the description above) it is expected that their behaviors are similar.

[37] Finally, the results for PC-OMD show an interesting symmetrical distribution between E, SE, S and W, NW, N, which is remarkably consistent with the meridional dipole of this pattern shown in Figure 4. When the PC-OMD has a positive index the E, SE, S circulation types are more common, and when PC-OMD has a negative index the W, NW, N circulation types prevail.

5. Nonstationarity of the Modes of Low-Frequency Variability in the NAE Sector and Their Influence on Circulation-Type Frequency

[38] In section 4, we identified the four NAE sector leading modes that affect the European climate in winter. Some studies have addressed the time variability of the effects of the modes. These works show that there are important changes in the relationship between atmospheric variables and these modes, in space as well as in time [*Krichak and Alpert*, 2005; *Beranová and Huth*, 2008; *Vicente-Serrano and López-Moreno*, 2008].

[39] In order to identify the temporal changes in position and intensity of modes, over the whole NAE sector (30°N–76°N and 37°W–56°E), we used a moving window PCA technique with a 30 year period for the winter months (JFM), thus yielding 29 subperiods of 30 years length covering the years 1948–2005. Thus, the first period of analysis was 1948–1977 (centered on 1962) and the last period was 1976–2005 (centered on 1990). From each period considered, we obtained the explained variance for the four leading modes together with the EOF pattern and its corresponding PC.

[40] The basic configuration of these modes remained the same, regardless of whether the analysis was stationary

Table 2. Correlation Between the Hemispheric Modes Time Series and the Frequency of the Synoptic Circulation Types in Winter[a]

Winter	Northeast	East	Southeast	South	Southwest	West	Northwest	North	Cyclonic	Anticyclonic
NAO	−0.13	−0.24	**−0.38**	−0.28	−0.03	0.18	−0.08	−0.06	**−0.61**	**0.54**
EA	−0.29	−0.09	−0.13	0.00	**0.52**	0.23	−0.27	**−0.40**	−0.12	−0.13
EA/WR	−0.16	0.23	**0.34**	0.17	0.28	**−0.49**	**−0.42**	−0.06	−0.09	0.23
SCA	0.12	0.08	−0.15	0.02	−0.01	0.17	0.31	0.23	**0.42**	**−0.50**

[a]Values in bold represent correlations that are statistically significant at the 99% level.

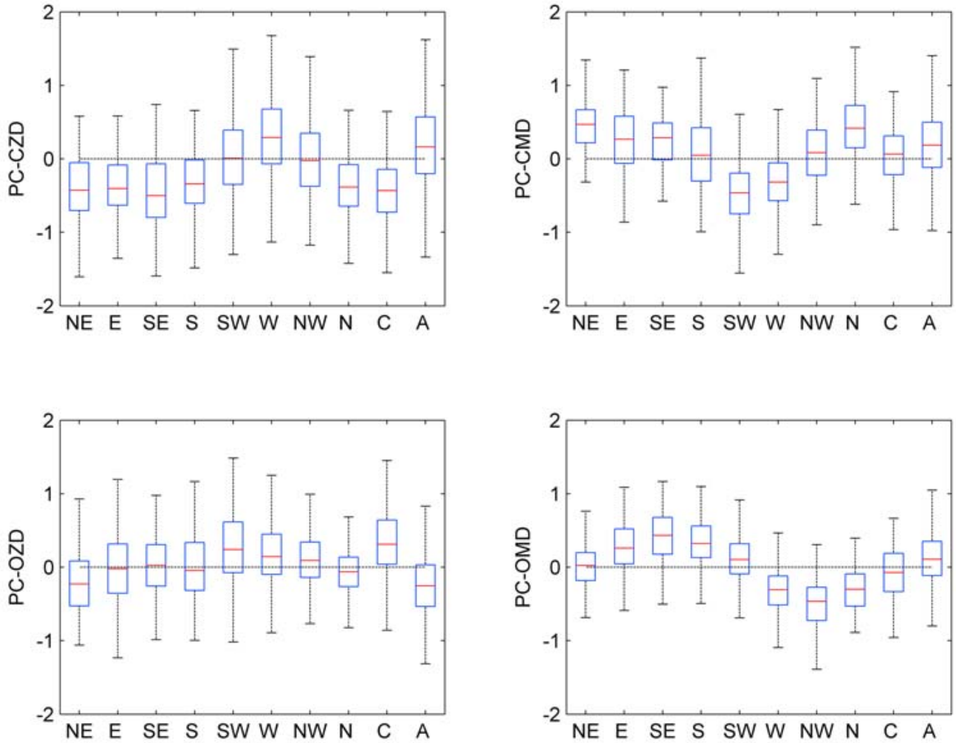

Figure 6. Distribution of the four corresponding principal component (PC) indices for each circulation type. The boxes represent the lower, median, and upper quartile values. The whisker lines are drawn at a scale of 1.5 times the interquartile range.

(section 4) or nonstationary (section 5). The dipoles remained the same, changing only in position or intensity (see below). We therefore use the same terminology for the EOF patterns and the corresponding loading factors as in section 4.

[41] The variance explained by each EOF over the period 1948–2004 for each 30 year window is represented in Figure 7. The most striking result is an increase in the explained variance of EOF1 (the CZD) from 27% in the first window to 32% in the last, this being consistently the leading mode in each of the 30 year windows. This increase is most obvious between 1952 and 1981 and 1962–1991. It is also very interesting to note that at the beginning of the period of analysis the CMD represents the second largest total variance, but over time this variance reduces (accompanied by an increase in variance accounted for by the CZD). After the 1956–1985 window, there are also some changes in order of the second and third most explained variance between the CMD and the OZD. It is worth stating that after the 1962–1991 window, for the most part the OZD represents the second largest variance. The contribution of the OMD shows no significant change over the period of analysis.

[42] Figure 8 shows the four leading modes in the region represented, using six selected 30 year time windows (1951–1980, 1956–1985, 1961–1990, 1966–1995, 1971–2000 and 1976–2005). Furthermore, we also analyze changes in the intensity of these modes (Figure 9). The intensity of the modes is given by doing the seasonal average (JFM) of the daily PCs of the modes computed in Figure 4. With this classical measure (time series of the PCA method) we can evaluate changes in the intensity of the modes and also the sign of the modes [*Jolliffe*, 2002]. The most obvious result is the eastward shift in the position of the CZD, with the positive (negative) action centers being located in the Azores (Iceland) region at the beginning of the first 30 year window (1948–1977) and in southern Iberia (Scandinavia) in the last 30 year window (1976–2005). These results are in line with those presented by *Ulbrich and Christoph* [1999] and *Vicente-Serrano and López-Moreno* [2008], who stated that the location of the NAO pattern undergoes multidecadal changes. This change in the CZD is less pronounced prior to the 1966–1995 window, but more pronounced thereafter. This result seems to support the work done by *Cassou et al.* [2004] and *Peterson et al.* [2003], who stated that the NAO might experience a significant eastward displacement toward Europe when it is in its positive phase and a westward shift during its negative phase. Furthermore, alongside this pronounced shift in the position of the CZD, there is also a step increase (significant at a 5% level) in its intensity, which is pronounced in the last 20 years (Figure 9).

[43] In the other modes (CMD, OZD, and OMD), there is no obvious shift in the positions of the dipoles. In reality, the OMD has three centers of action, with two negative centers to the west and east of central Europe, and a positive center in central Europe, but because our area of interest is located in the western part of the region, we focus on the left side of these centers of action. In this case, it seems there is a very slight increase in the positive part of the tripole, pushing the left (negative) part of the tripole further west.

[44] Despite the absence of any obvious shifts in the position of these modes (CMD, OZD and OMD), there are some interesting points to note in terms of the changes in their intensities (Figure 9). For the intensities, we also determined

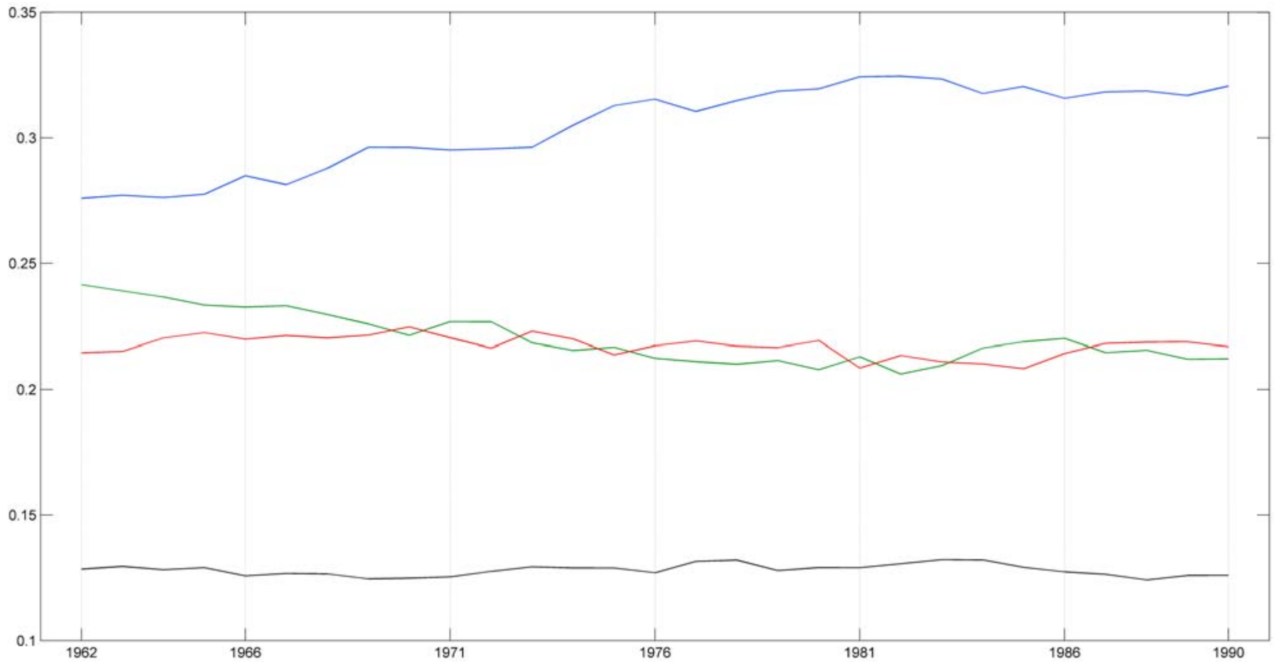

Figure 7. Variance explained by each EOF over time. The first analysis window is 1948–1977 (centered on 1962) and the last is 1976–2005 (centered on 1990). The continental zonal dipole (CZD), continental meridional dipole (CMD), ocean zonal dipole (OZD), and ocean meridional dipole (OMD) are represented by the blue, green, red, and black lines, respectively.

whether changes described below are significant by performing a *t* student test. For all period the analysis the PC-CZD show an increase in their intensity significant at a 5% level. On the PC-CMD, there is almost any change in the intensity and signal. On the contrary, the PC-OZD shows an initial increment but in the final 3 decades there is a high decrease in the PC of this mode (significant at 5% level). Finally, the PC-OMD appears to have a very slight increase in intensity (not significant at a 5% level).

[45] Having studied the changes in the position and intensity of the four NAE sector leading modes that affect Europe and our study area in particular, we wished to determine the effects of these changes on the local circulation patterns. In order to achieve this, we computed the correlation between the four leading principal components of the PCA (using the 29 subperiods of 30 years length time windows) and the respective seasonal frequency of circulation type (Figure 10).

[46] When we analyzed Figure 3 the striking result was that there were circulation types that in winter had low frequency, especially the ones on the 1st and 2nd quadrants (NE, E, SE, S, and N). Each of these type represent, in average, less than 5 d per winter, and so should be treated with caution, despite some significant changes being apparent. Therefore, we do not discuss them in this section. For the main changes in the correlation coefficients (SW, NW, and A types) we also computed a significance test (*t* student test for the linear trends and a Mann-Whitney test when a step change occurs).

[47] The most frequent anticyclonic circulation type (which produces virtually no rain in Galicia) and the next four most frequent circulation types (SW, W, NW, and cyclonic) (which together explain almost all of the precipitation in Galicia [*Lorenzo et al.*, 2008]), require further discussion. For the SW circulation type, it may be seen that the correlation between the PC-OZD and the frequency of this circulation type is always positive, but starts to decrease linearly after 1970, changing over time from being significant to nonsignificant. This change in the correlation coefficient is significant at a 5% level. Since there is no change in the position of this mode (OZD), this phenomenon may be attributed to changes in the intensity of its associated dipole. In fact, there is an increase in the intensity of this mode up to 1980 followed by a step decrease (Figure 9). The OZD mode in the Iberia Peninsula is characterized by a SW/NW flow (Figure 8), depending of the signal of the intensity (positive/negative) of the mode. Therefore, it is expectable that the correlation between PC-OZD and the frequency of SW type decreases when the intensity of the OZD mode tends to negative values. For the other modes (CZD, CMD, and OMD), there are no obvious changes in the correlation to speak of.

[48] It may be seen that for the W circulation type, there are no particular changes in the correlation with the EOF loading factors. The only exception to this is the decrease in the correlation with PC-OMD, with a minimum (nonsignificant correlation) at 1967. Over time, however, this correlation increases and is statistically significant for almost the entire period of analysis. In fact, it seems that changes in the intensity (toward positive values) of the OMD are correlated negatively with changes in the frequency of the W type.

[49] For the NW circulation type, there is a striking change in behavior concerning PC-CZD (PC-OZD) where a positive (negative) correlation may be seen prior to 1976, with a negative (positive) correlation after 1976. Furthermore, the correlation in the final window seems to be more significant, with values greater than 95%. By comparing the NW type (Figure 2) and the CZD in the first few time windows (Figure 8), it may be seen that they are very similar. This

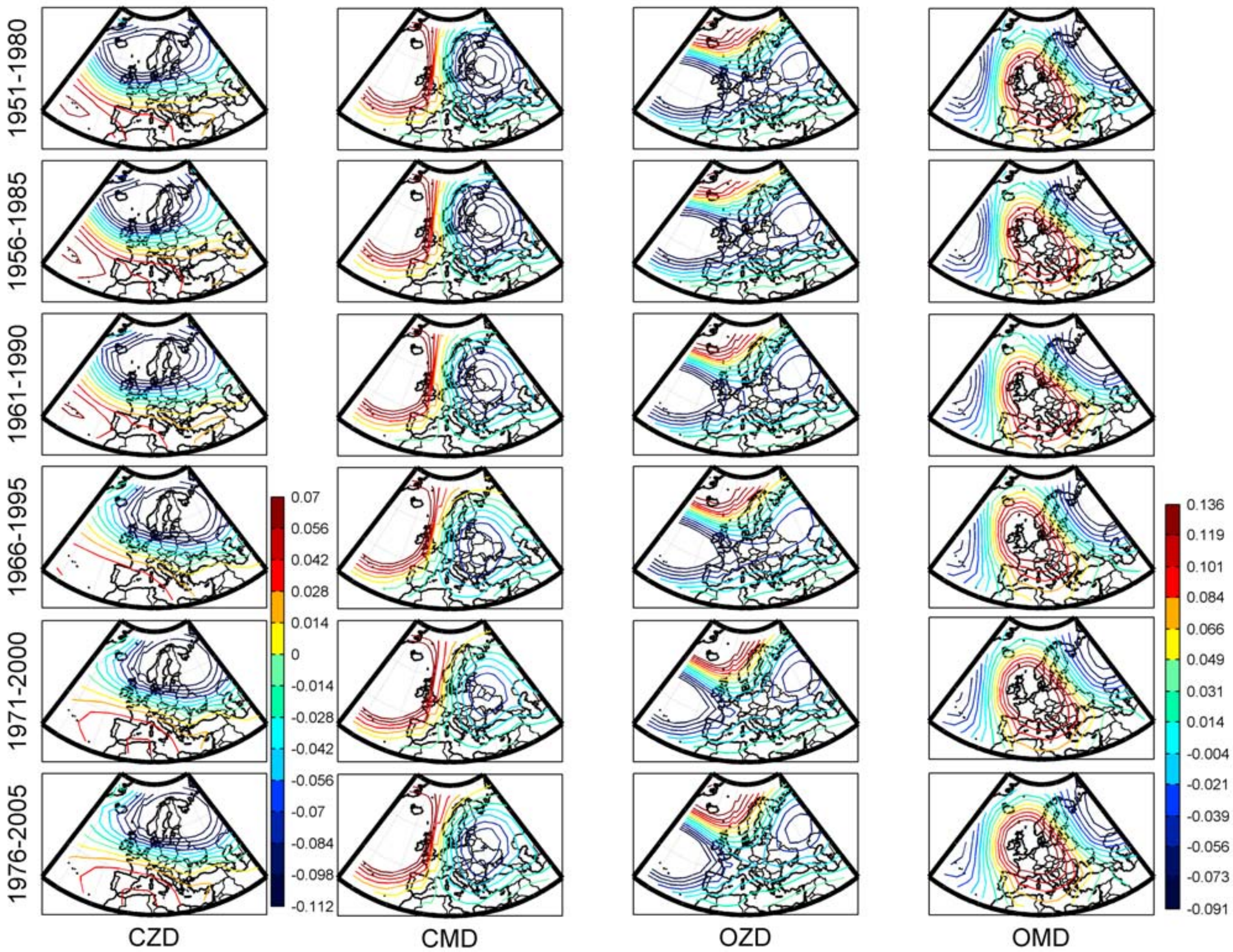

Figure 8. The first four leading EOF patterns for the winter months (JFM) obtained using a principal component analysis on the SLP field using a 30 year moving window.

could help to explain the significant positive correlation with the frequency of this circulation type. Over time, the shift of the CZD toward Europe has a negative influence on the frequency with which this circulation type occurs. In the case of the OZD, it seems that there is an increase in the intensity of this mode up to the 1965 alongside with a decrease in the correlation between PC-OZD and the frequency of the NW type. By the time there is a change in the intensity of the OZD (toward more negative values), the correlation between the frequency of the NW type and PC-OZD changes from negative values to positive values. In addition, these (trend) changes in the correlation coefficient are also significant at a 5% level. As we explained for the SW type (but with an opposite behavior in the NW type) it is expectable that, the correlation between PC-OZD and the frequency of NW type increases when the intensity of the OZD mode tends to negative values.

[50] For the cyclonic circulation type, an increase of the anticorrelation (significant in all periods of analysis) with PC-CZD may be observed for the last 15 time windows. This is most probably derived from the eastward shift (especially at that time) of the position of the first mode (Figure 8), blocking the storm track in the region. Furthermore, there is a slight increase in the correlation (always significant) with PC-OZD after 1967. The (significant) anticorrelation between the cyclonic type and PC-OMD shows a slight decrease over the whole period.

[51] Focusing on the correlation between the frequency of anticlyclonic circulation type and the EOF loadings, there is a strong resemblance between the correlation for this circulation type and PC-CZD and PC-OZD (but with the opposite sign). With the eastward shift of the CZD center of action close to the region, its influence increases, not only on the cyclonic type but also on the anticyclonic type, as the results seem to indicate. There is also an interesting result for the CMD mode, with a decreasing correlation with the anticyclonic type (an important decrease in the correlation coefficient significant at a 5% level). It is interesting to note that the curve of correlation between the PC-CMD and the frequency of anticlyclonic circulation are alike to the curve of the CMD intensity.

6. Conclusions

[52] We have herein described the compatibility between hemispheric modes and modes in NAE sector, using the local

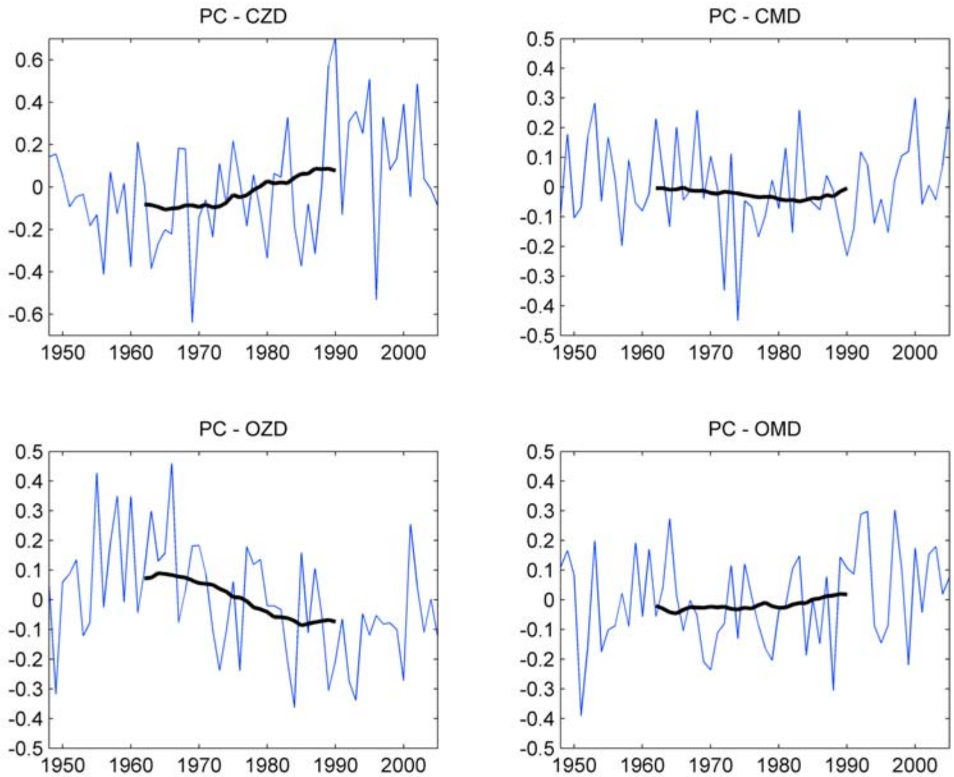

Figure 9. Intensity of the modes given by doing the seasonal average (JFM) of the daily PCs of the modes represented in Figure 4. The 30 year moving average is also represented (black lines).

circulation regimes of a specific study area, namely those found in the northwest Iberian Peninsula for winter months (JFM). We have provided evidence that the modes computed using the SLP field or the H500 field are very alike in this spatial window. The results show that there is a high degree of coherence between the modes derived from a statistical approach (using PCA) and the real physical circulations (as represented by the circulation types). This coherence was obtained not only when we used stationary modes, but also with nonstationary ones. The use of a PCA approach using continuous time windows has enabled us to assess whether changes in the intensity or position of these modes could influence the local circulation. The results confirm that changes in both the position and the intensity of the modes tend to favor the occurrence of some circulation types in preference to others. Again, these changes are coherent and consistent.

[53] The most important results are as follows:

[54] 1. Correlation coefficients obtained between hemispheric modes and the frequencies of 10 circulation types during winter show that the NAO pattern yields the greatest correlation with the cyclonic and anticyclonic circulation type, these types being responsible for higher and lower precipitation in the Iberian Peninsula, respectively. The EA pattern has a significantly high correlation with the SW circulation type. The EA/WR pattern shows a significant correlation with the W and the NW circulation types. Finally, the SCA pattern exhibits the opposite behavior from the NAO, with a negative correlation with the anticyclonic circulation type and a positive correlation with the cyclonic. It is interesting to note that these types occur at a high frequency during winter (more than 60% of the total frequency).

[55] 2. By studying the compatibility between local circulation type classification and modes in NAE sector, we found that, for the winter months (JMF), the zonal dipoles (continental and ocean) have a major influence, not only on the occurrence of the cyclonic and anticyclonic circulation type, but also on the zonal types. As expected, the meridional dipoles influence the circulation types that are related to meridional circulations, such as the E and W circulation types.

[56] 3. We have also shown how changes in the position and intensity of modes over the last 50 years have influenced the local circulation in our study area. There is an increase in the explained variance of the continental zonal dipole from 27% in the first time window to 32% in the final one. There is also an eastward shift in the position of this mode, which is in agreement with the findings of *Ulbrich and Christoph* [1999] and *Vicente-Serrano and López-Moreno* [2008], along with an increase in its intensity. For the other modes, namely the ocean zonal dipole and the two meridional ones, no obvious shifts in their positions were found.

[57] In summary, we have identified relationships between the real physical local circulations (as represented by circulation type) and the modes obtained from statistical analysis. Changes in the positions and intensities of these modes have an impact on the local circulation (here assessed by the circulation type) for our target area. The increase in explained variance of the continental zonal dipole and the increasing negative (positive) correlation between this mode and the cyclonic (anticyclonic) circulation type can help to explain

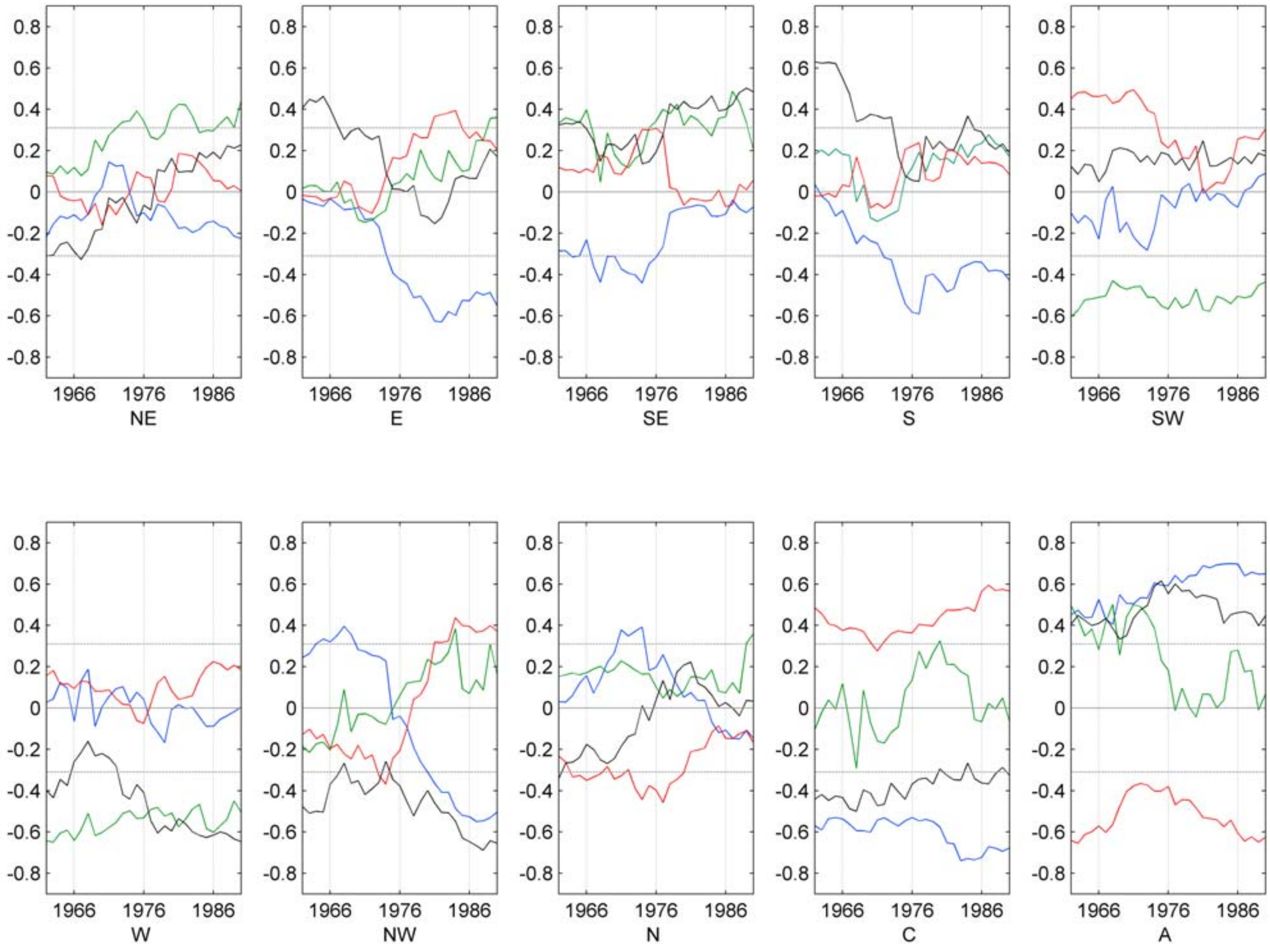

Figure 10. Correlation between the four principal loading factors and the winter frequency of the circulation types. The significance at the 95% level is also shown (dotted lines). The first analysis window is set as 1948–1977 (centered on 1962), and the last window is set as 1976–2005 (centered on 1990). Cyclonic and anticyclonic are denoted by C and A, respectively. The CZD, CMD, OZD, and OMD are represented by blue, green, red, and black lines, respectively.

the overall decrease of precipitation in winter [*Paredes et al.*, 2006; *Trigo et al.*, 2008] in the study region.

Appendix A

A1. Definition of Circulation Type in Galicia (NW Spain)

[58] Here we used the results for daily circulation types for Galicia computed by *Lorenzo et al.* [2008] which adopted the classification types of *Jenkinson and Collison* [1977] and *Jones et al.* [1993] for weather circulation.

[59] The weather conditions were determined using physical or geometrical considerations, such as the direction and strength of airflow, and degree of cyclonicity. The indices used were the following: southerly flow (SF), westerly flow (WF), total flow (F), southerly shear vorticity (ZS), westerly shear vorticity (ZW), and total shear vorticity (Z) were computed using SLP values obtained for the 16 grid points (p1–p16), as shown in Figure 1. These points were moved 5° to the north compared with the study of *Trigo and DaCamara* [2000], in order to center our area in the grid. Reanalysis data for the SLP that were obtained from the National Center for Atmospheric Research were used to obtain the daily SLP covering the winter period (JFM) from 1948 to 2005. We used the following expressions when calculating the indices:

$$\mathrm{SF} = 1.305[0.25(\mathrm{p5} + 2\mathrm{p9} + \mathrm{p13}) - 0.25(\mathrm{p4} + 2\mathrm{p8} + \mathrm{p12})]$$

$$\mathrm{WF} = [0.5(\mathrm{p12} + \mathrm{p13}) - 0.5(\mathrm{p4} + \mathrm{p5})]$$

$$\mathrm{ZS} = 0.85[0.25(\mathrm{p6} + 2\mathrm{p10} + \mathrm{p14}) - 0.25(\mathrm{p5} + 2\mathrm{p9} + \mathrm{p13}) - 0.25(\mathrm{p4} + 2\mathrm{p8} + \mathrm{p12}) + 0.25(\mathrm{p3} + 2\mathrm{p7} + \mathrm{p11})]$$

$$\mathrm{ZW} = 1.12[0.5(\mathrm{p15} + \mathrm{p16}) - 0.5(\mathrm{p8} + \mathrm{p9})] - 0.91[0.5(\mathrm{p8} + \mathrm{p9}) - 0.5(\mathrm{p1} + \mathrm{p2})]$$

$$\mathrm{F} = (\mathrm{SF2} + \mathrm{WF2})1/2$$

$$\mathrm{Z} = \mathrm{ZS} + \mathrm{ZW}$$

[60] The conditions established to define different types of circulation are the same as those of *Trigo and DaCamara* [2000], and the following set rules were used:

[61] 1. Direction of flow was given by tan-1(WF/SF), 180° being added if WF was positive. The appropriate direction

was computed using an eight-point compass, allowing 45° per sector.

[62] 2. If $|Z| < F$, the flow is essentially straight and was considered to be of a pure directional type (eight different cases, according to the directions of the compass).

[63] 3. If $|Z| > 2F$, the pattern was considered to be of a pure cyclonic type if $Z > 0$, or of a pure anticyclonic type if $Z < 0$.

[64] 4. If $F < |Z| < 2F$, the flow was considered to be of a hybrid type and was therefore characterized by both direction and circulation (8×2 different types).

[65] These rules allow 26 different types of weather. However, in this study we use only the 10 "pure" weather types (NE, E, SE, S, SW, W, NW, N, C, and A).

A2. Definition of the Modes of Low-Frequency Variability

[66] The modes of low-frequency variability in the NAE sector were computed using a PCA technique. This technique was first applied to the daily winter (JFM) SLP field for the whole period of analysis (1948–2005) and taking into account the NAE sector (30°N–76°N and 37°W–56°E). The covariance matrix was created using the time values at each grid point. This corresponds to a PCA in S mode (using the terminology of *Richman* [1986]), which means that the eigenvector describes the spatial pattern of the modes of low-frequency variability and the principal components (PCs) describe the time variations (in our case the indices of the low-frequency variability modes in NAE sector). Because of the fact that our grid covers an area between 30°N and 76°N, each grid cell in the data is the same size, but each grid cell on the Earth is a different size, according to its latitude. In order to ensure the equality in the grid areas, the gridded data were weighted by the square root of the cosine of latitude [*Chung and Nigam*, 1999]. Finally, a Varimax orthogonal rotation was also applied. The same methodology was also applied to the daily 500 hPa geopotential height field (H500).

[67] **Acknowledgments.** This work is supported by "Xunta de Galicia" under project PGIDIT06PXIB383288PR. Nieves Lorenzo acknowledges the support by the Ramon y Cajal program. Alexandre M. Ramos was supported through Portuguese Science Foundation (FCT) through grant BD/46000/2008. Finally the authors would like to thank both reviewers for their helpful and constructive comments that help in improving the manuscript.

References

Barnston, A. G., and R. E. Livezey (1987), Classification, seasonality and persistence of low-frequency atmospheric circulation patterns, *Mon. Weather Rev.*, *115*, 1083–1126, doi:10.1175/1520-0493(1987)115<1083:CSAPOL>2.0.CO;2.

Beranová, R., and R. Huth (2007), Time variations of the relationships between the North Atlantic Oscillation and European winter temperature and precipitation, *Stud. Geophys. Geod.*, *51*, 575–590, doi:10.1007/s11200-007-0034-3.

Beranová, R., and R. Huth (2008), Time variations of the effects of circulation variability modes on European temperature and precipitation in winter, *Int. J. Climatol.*, *28*, 139–158, doi:10.1002/joc.1516.

Blackburn, M., and B. J. Hoskins (2001), The UK record-breaking wet autumn 2000, *UGAMP Newsl.*, *24*, 38–40.

Bojariu, R., and L. Gimeno (2003), Predictability and numerical modelling of the North Atlantic Oscillation, *Earth Sci. Rev.*, *63*, 145–168, doi:10.1016/S0012-8252(03)00036-9.

Cassou, C., T. Laurent, J. W. Hurrell, and C. Deser (2004), North Atlantic winter climate regimes: Spatial asymmetry, stationarity with time and oceanic forcing, *J. Clim.*, *17*, 1055–1068, doi:10.1175/1520-0442(2004)017<1055:NAWCRS>2.0.CO;2.

Chen, D., and C. Hellström (1999), The influence of the North Atlantic Oscillation on the regional temperature variability in Sweden: Spatial and temporal variations, *Tellus*, *51A*, 505–516.

Chung, C., and S. Nigam (1999), Weighting of geophysical data in principal component analysis, *J. Geophys. Res.*, *104*(D14), 16,925–16,928, doi:10.1029/1999JD900234.

Corte-Real, J., X. Zhangzheng, and X. Wang (1995), Large-scale circulation regimes and surface climatic anomalies over the Mediterranean, *Int. J. Climatol.*, *15*, 1135–1150, doi:10.1002/joc.3370151006.

Corte-Real, J., B. Qian, and H. Xu (1999), Circulation patterns, daily precipitation in Portugal and implications for climate change simulated by the second Hadley Centre GCM, *Clim. Dyn.*, *15*, 921–935, doi:10.1007/s003820050322.

deCastro, M., M. N. Lorenzo, J. J. Taboada, M. Sarmiento, I. Álvarez, and M. Gomez-Gesteira (2006), Teleconnection patterns influence on precipitation variability and on river flow regimes in the Miño River basin (NW Iberian Peninsula), *Clim. Res.*, *32*, 63–73, doi:10.3354/cr032063.

deCastro, M., M. Gómez-Gesteira, M. N. Lorenzo, I. Álvarez, and A. J. C. Crespo (2008), Influence of atmospheric modes on coastal upwelling along the western coast of the Iberian Peninsula, 1985 to 2005, *Clim. Res.*, *36*, 169–179, doi:10.3354/cr00742.

Dunkeloh, A., and J. Jacobeit (2003), Circulation dynamics of Mediterranean precipitation variability 1948–98, *Int. J. Climatol.*, *23*, 1843–1866, doi:10.1002/joc.973.

Garcia-Herrera, R., E. Hernández, D. Barriopedro, D. Paredes, R. M. Trigo, I. F. Trigo, and M. A. Mendes (2007), The outstanding 2004/05 drought in the Iberian Peninsula: Associated atmospheric circulation, *J. Hydrometeorol.*, *8*, 483–498, doi:10.1175/JHM578.1.

Gimeno, L., L. de la Torre, R. Nieto, R. García, E. Hernández, and P. Ribera (2003), Changes in the relationship NAO–Northern hemisphere temperature due to solar activity, *Earth Planet. Sci. Lett.*, *206*, 15–20, doi:10.1016/S0012-821X(02)01090-7.

Glowienka-Henze, R. (1990), The North Atlantic Oscillation in the Atlantic-European SLP, *Tellus*, *42A*, 497–507.

Goodess, C. M., and J. P. Palutikof (1998), Development of daily rainfall scenarios for southeast Spain using a circulation-type approach to downscaling, *Int. J. Climatol.*, *18*, 1051–1083, doi:10.1002/(SICI)1097-0088(199808)18:10<1051::AID-JOC304>3.0.CO;2-1.

Hurrell, J. W., and H. van Loon (1997), Decadal variations associated with the North Atlantic Oscillation, *Clim. Change*, *36*, 301–326, doi:10.1023/A:1005314315270.

Hurrell, J. W., Y. Kushnir, M. Visbeck, and G. Ottersen (2003), An overview of the North Atlantic Oscillation, in *The North Atlantic Oscillation: Climate Significance and Environmental Impact*, *Geophys. Monogr. Ser.*, vol. 134, edited by J. W. Hurrell et al., pp. 1–36, AGU, Washington, D. C.

Huth, R. (2006), The effect of various methodological options on the detection of leading modes of sea level pressure variability, *Tellus*, *58A*, 121–130.

Huth, R., C. Beck, A. Philipp, M. Demuzere, Z. Ustrnul, M. Cahynová, J. Kysely, and O. E. Tveito (2008), Classifications of atmospheric circulation patterns: Recent advances and applications, in *Trends and Directions in Climate Research*, *Ann. N. Y. Acad. Sci.*, *1146*, 105–152, doi:10.1196/annals.1446.019.

Intergovernmental Panel on Climate Change (2007), *Climate Change 2007: The Physical Science Basis, Contribution of Working Group I to the Fourth Assessment Report of the Intergovernmental Panel on Climate Change*, edited by S. Solomon et al., Cambridge Univ. Press, Cambridge, U. K.

Jenkinson, A. F., and F. P. Collison (1977), An initial climatology of gales over the North Sea, *Synoptic Climatol. Branch Memo. 62*, Meteorol. Off., Bracknell, U. K.

Jolliffe, I. T. (1990), Principal component analysis: A beginner's Guide. Part I: Introduction and application, *Weather*, *45*, 375–382.

Jolliffe, I. T. (2002), *Principal Component Analysis*, 2nd ed., Springer, New York.

Jones, P. D., M. Hulme, and K. R. Briffa (1993), A comparison of Lamb circulation types with an objective classification scheme, *Int. J. Climatol.*, *13*, 655–663, doi:10.1002/joc.3370130606.

Jones, P. D., T. J. Osborn, and K. R. Briffa (2003), Pressure-based measures of the North Atlantic Oscillation (NAO): A comparison and an assessment of changes in the strength of the NAO and in its influence on surface climate parameters, in *The North Atlantic Oscillation: Climate Significance and Environmental Impact*, *Geophys. Monogr. Ser.*, vol. 134, edited by J. W. Hurrel et al., pp. 51–62, AGU, Washington, D. C.

Jung, T., M. Hilmer, E. Ruprecht, S. Kleppek, S. K. Gulev, and O. Zolina (2003), Characteristics of the recent eastward shift of interannual NAO variability, *J. Clim.*, *16*, 3371–3382, doi:10.1175/1520-0442(2003)016<3371:COTRES>2.0.CO;2.

Kalnay, E., et al. (1996), The NCEP/NCAR 40-Year Reanalysis Project, *Bull. Am. Meteorol. Soc.*, *77*(3), 437–471.

Krichak, S., and P. Alpert (2005), Decadal trends in the east Atlantic-west Russia pattern and the Mediterranean precipitation, *Int. J. Climatol.*, *25*, 183–192, doi:10.1002/joc.1124.

Lorenzo, M. N., and J. J. Taboada (2005), Influences of atmospheric variability on freshwater input in Galician Rías in winter, *J. Atmos. Ocean Sci.*, *10*, 377–387, doi:10.1080/17417530601127472.

Lorenzo, M. N., J. J. Taboada, and L. Gimeno (2008), Links between circulation weather types and teleconnection patterns and their influence on precipitation patterns in Galicia (NW Spain), *Int. J. Climatol.*, *28*, 1493–1505, doi:10.1002/joc.1646.

Lu, J., and R. J. Greatbatch (2002), The changing relationship between the NAO and northern hemisphere climate variability, *Geophys. Res. Lett.*, *29*(7), 1148, doi:10.1029/2001GL014052.

Paredes, D., R. M. Trigo, R. Garcia-Herrera, and I. F. Trigo (2006), Understanding precipitation changes in Iberia in early spring: Weather typing and storm-tracking approaches, *J. Hydrometeorol.*, *7*, 101–113, doi:10.1175/JHM472.1.

Peterson, K. A., J. Lu, and R. J. Greatbatch (2003), Evidence of nonlinear dynamics in the eastward shift of the NAO, *Geophys. Res. Lett.*, *30*(2), 1030, doi:10.1029/2002GL015585.

Richman, M. B. (1986), Rotation of principal components, *J. Climatol.*, *6*, 293–335, doi:10.1002/joc.3370060305.

Rodríguez-Puebla, C., A. H. Encinas, S. Nieto, and J. Garmendia (1998), Spatial and temporal patterns of annual precipitation variability over the Iberian Peninsula, *Int. J. Climatol.*, *18*, 299–316, doi:10.1002/(SICI)1097-0088(19980315)18:3<299::AID-JOC247>3.0.CO;2-L.

Sáenz, J., C. Rodríguez-Puebla, J. Fernández, and J. Zubillaga (2001), Interpretation of interannual winter temperature variations over southwestern Europe, *J. Geophys. Res.*, *106*(D18), 20,641–20,651, doi:10.1029/2001JD900247.

Slonosky, V. C., P. D. Jones, and T. D. Davies (2001), Atmospheric circulation and surface temperature in Europe from the 18th century to 1995, *Int. J. Climatol.*, *21*, 63–75, doi:10.1002/joc.591.

Trigo, I. F. (2005), Climatology and interannual variability of storm-tracks in the Euro-Atlantic sector: A comparison between ERA-40 and NCEP/NCAR reanalyses, *Clim. Dyn.*, *26*, 127–143, doi:10.1007/s00382-005-0065-9.

Trigo, R. M., and C. C. DaCamara (2000), Circulation weather types and their influence on the precipitation regime in Portugal, *Int. J. Climatol.*, *20*, 1559–1581, doi:10.1002/1097-0088(20001115)20:13<1559::AID-JOC555>3.0.CO;2-5.

Trigo, R. M., and J. P. Palutikof (2001), Precipitation scenarios over Iberia: A comparison between direct GCM output and different downscaling techniques, *J. Clim.*, *14*, 4422–4446, doi:10.1175/1520-0442(2001)014<4422:PSOIAC>2.0.CO;2.

Trigo, R. M., T. J. Osborn, and J. M. Corte-Real (2002), The North Atlantic Oscillation influence on Europe: Climate impacts and associated physical mechanisms, *Clim. Res.*, *20*, 9–17, doi:10.3354/cr020009.

Trigo, R. M., M. A. Valente, I. F. Trigo, P. M. A. Miranda, A. M. Ramos, D. Paredes, and R. García-Herrera (2008), The impact of North Atlantic wind and cyclone trends on European precipitation and significant wave height in the Atlantic, in *Trends and Directions in Climate Research*, *Ann. N. Y. Acad. Sci.*, *1146*, 212–234, doi:10.1196/annals.1446.014.

Ulbrich, U., and M. Christoph (1999), A shift of the NAO and increasing storm track activity over Europe due to anthropogenic greenhouse gas forcing, *Clim. Dyn.*, *15*, 551–559, doi:10.1007/s003820050299.

Vicente-Serrano, S. M., and J. I. López-Moreno (2008), Nonstationary influence of the North Atlantic Oscillation on European precipitation, *J. Geophys. Res.*, *113*, D20120, doi:10.1029/2008JD010382.

Wallace, J. M., and D. S. Gutzler (1981), Teleconnections in the geopotential height field during the Northern Hemisphere winter, *Mon. Weather Rev.*, *109*, 784–812, doi:10.1175/1520-0493(1981)109<0784:TITGHF>2.0.CO;2.

Walter, K., and H.-F. Graf (2002), On the changing nature of the regional connection between the North Atlantic Oscillation and sea surface temperature, *J. Geophys. Res.*, *107*(D17), 4338, doi:10.1029/2001JD000850.

Wibig, J. (1999), Precipitation in Europe in relation to circulation patterns at the 500 hpa level, *Int. J. Climatol.*, *19*, 253–269, doi:10.1002/(SICI)1097-0088(19990315)19:3<253::AID-JOC366>3.0.CO;2-0.

Zveryaev, I. I. (2006), Seasonally varying modes in long-term variability of European precipitation during the 20th century, *J. Geophys. Res.*, *111*, D21116, doi:10.1029/2005JD006821.

L. Gimeno, M. N. Lorenzo, and A. M. Ramos, EPHYSLAB, Faculty of Sciences, University of Vigo, Campus de Ourense, E-32004 Ourense, Spain. (alexramos@uvigo.es)